



Contents lists available at ScienceDirect

## Saudi Journal of Biological Sciences

journal homepage: [www.sciencedirect.com](http://www.sciencedirect.com)

Original article

## Development of antidiabetic drugs from benzamide derivatives as glucokinase activator: A computational approach

Amena Ali

Department of Pharmaceutical Chemistry, College of Pharmacy, Taif University, P.O. Box 11099, Taif 21944, Saudi Arabia



## ARTICLE INFO

## Article history:

Received 18 July 2021

Revised 27 January 2022

Accepted 30 January 2022

Available online 4 February 2022

## Keywords:

Glucokinase activator

Benzamide

3D-QSAR

Virtual screening

Pharmacophore analysis

Docking

## ABSTRACT

Hyperglycemia is a condition known for the impairment of insulin secretion and is responsible for diabetes mellitus. Various small molecule inhibitors have been discovered as glucokinase activators. Recent studies on benzamide derivatives showed their importance in the treatment of diabetes as glucokinase activator. The present manuscript showed a computation study on benzamide derivatives to help in the production of potent glucokinase activators. In the present study, pharmacophore development, 3D-QSAR, and docking studies were performed on benzamide derivatives to find out the important features required for the development of a potential glucokinase activator. The generated pharmacophore hypothesis ADRR\_1 consisted of essential features required for the activity. The resultant statistical data showed high significant values with  $R^2 > 0.99$ ; 0.98 for the training set and  $Q^2 > 0.52$ ; 0.71 for test set based on atom-based and field-based models, respectively. The potent compound 15b of the series showed a good docking score via binding with different amino acid residues such as (NH...ARG63), (SO<sub>2</sub>...ARG250, THR65), and  $\pi$ - $\pi$  staking with (phenyl...TYR214). The virtual screening study used 3563 compounds from ZINC database and screened hit compound ZINC08974524, binds with similar amino acids as shown by compound 15b and crystal ligand with docking scores SP (-11.17 kcal/mol) and XP (-8.43 kcal/mol). Compounds were further evaluated by ADME and MMGBSA parameters. Ligands and ZINC hits showed no violation of Lipinski rules. All the screened compounds showed good synthetic accessibility. The present study may be used by researchers for the development of novel benzamide derivatives as glucokinase activator.

© 2022 The Author. Published by Elsevier B.V. on behalf of King Saud University. This is an open access article under the CC BY license (<http://creativecommons.org/licenses/by/4.0/>).

## 1. Introduction

Glucokinase is a hexokinase isozyme, consist of 465 amino acids (molecular weight = 50 kD) present in pancreatic  $\beta$ -cells and liver (postprandial state). Glucokinase catalyzes a reaction that involve the transfer of phosphate from ATP to glucose and the generation of glucose 6-phosphate which is the first step in the direction of synthesis of glycogen and glycolysis (Matschinsky 1996; Antoine and Boutin 2009). This reaction is also representing the first rate-limiting step in glucose metabolism. Glucokinase activator (GK-A) worked through two different mechanisms known as lowering the blood glucose level in the liver and increasing insulin secretion

in pancreatic  $\beta$ -cells. Therefore, it becomes an interesting target in the present scenario to treat diabetes. Various GK-As have been synthesized, some are under clinical studies and showed promising results to lower blood glucose levels in healthy people and type-2 diabetes mellitus (T2-DM) patients. Glucokinase activator is responsible for several side effects such as hypoglycemia and testicular toxicity (American Diabetes Association 2009; Waring et al. 2011). To eliminate these side effects, frequent dose regimens and dose titration are preferred. There are two different approaches described to treat hypoglycemic state, one is related to the designing of partial activators (Pfefferkorn et al. 2011) and the second approach is to restrict liver-selective glucose activators (Beberitz et al. 2009; Massa et al. 2011; Pfefferkorn et al. 2012; Park 2012; Park et al. 2013).

In the direction to treat diabetes, various benzamide derivatives have been developed as GK-As (Matschinsky et al. 2010; Mao et al., 2012). Park, et al. identified a novel phenylethyl benzamide GK-A (Park 2012; Park et al. 2013). Furthermore, Park et al. synthesized a series of pyrazole benzamide derivatives as GK-A having 3-methylpyridine and 4-phenoxyethyl sulfone groups for the treat-

Peer review under responsibility of King Saud University.

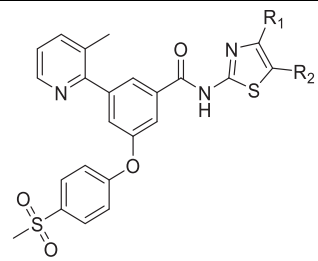
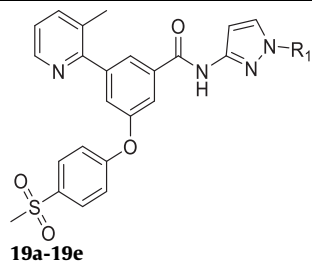
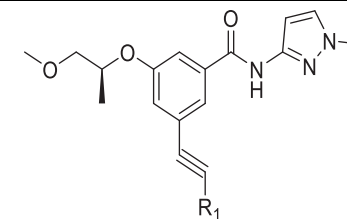


Production and hosting by Elsevier

E-mail address: [amrathore@tu.edu.sa](mailto:amrathore@tu.edu.sa)<https://doi.org/10.1016/j.sjbs.2022.01.058>

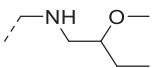
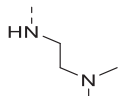
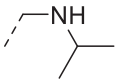
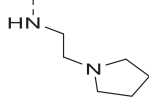
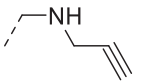
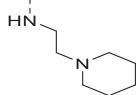
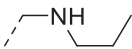
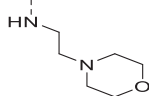
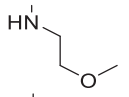
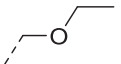
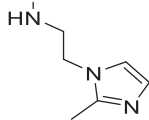
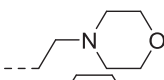
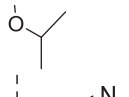
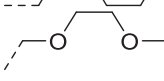
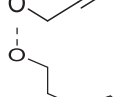
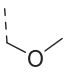
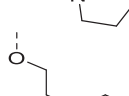
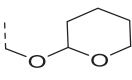
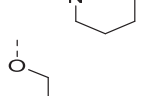
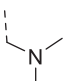
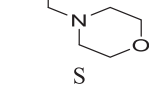
1319-562X/© 2022 The Author. Published by Elsevier B.V. on behalf of King Saud University.

This is an open access article under the CC BY license (<http://creativecommons.org/licenses/by/4.0/>).

**Table 1**In vitro IC<sub>50</sub> and pIC<sub>50</sub> values for GK activity of pyrazole benzamide derivatives (Park 2012; Park et al. 2013).**15a-18k****19a-19e****13a1-22e1**

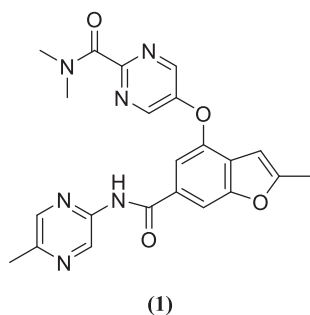
C	R1	R2	AP-A (IC <sub>50</sub> , μM)	AP-A (pIC <sub>50</sub> )	C	R1	R2	AP-A (IC <sub>50</sub> , μM)	AP-A (pIC <sub>50</sub> )
<b>16a</b>	H	H	0.095	7.02	<b>16b1</b>		-	0.301	6.52
<b>16b</b>	H	F	0.238	6.62	<b>16c1</b>		-	0.025	7.60
<b>15a</b>		H	0.103	6.99	<b>18a1</b>		-	0.021	7.68
<b>15b</b>		H	0.005	8.30	<b>18b1</b>		-	0.012	7.92
<b>18a</b>		H	50	4.30	<b>18c1</b>		-	0.03	7.52
<b>18b</b>		H	0.212	6.67	<b>18d1</b>		-	0.034	7.47
<b>18c</b>		H	0.688	6.16	<b>19</b>		-	0.027	7.57
<b>18d</b>		H	2.43	5.61	<b>21</b>		-	0.039	7.41
<b>18e</b>		H	7.46	5.13	<b>20a1</b>		-	0.037	7.43
<b>18f</b>		H	50	4.30	<b>20b1</b>		-	0.163	6.79
<b>18 g</b>		H	0.008	8.10	<b>20c1</b>		-	0.006	8.22

Table 1 (continued)

<b>18 h</b>		H	0.033	7.48	<b>20d1</b>		-	0.006	8.22
<b>18 i</b>		H	0.463	6.33	<b>20e1</b>		-	0.006	8.22
<b>18 j</b>		H	0.106	6.97	<b>20f1</b>		-	0.02	7.70
<b>18 k</b>		H	50	4.30	<b>20 g1</b>		-	0.039	7.41
<b>19 a</b>	CH <sub>3</sub>	-	0.807	6.09	<b>20 h1</b>		-	0.009	8.05
<b>19 b</b>		-	50	4.30	<b>22a1</b>		-	0.053	7.28
<b>19 d</b>		-	0.441	6.36	<b>22b1</b>		-	0.046	7.34
<b>19 e</b>		-	0.315	6.50	<b>22c1</b>		-	0.006	8.22
<b>13 a1</b>		-	1.87	5.73	<b>22d1</b>		-	0.007	8.15
<b>13 b1</b>		-	0.006	8.22	<b>22e1</b>		-	0.016	7.80
<b>16 a1</b>		-	7.7	5.11					

C: Compound; AP-A: Antiproliferative activity.

ment of T2-DM. Grewal *et al.* synthesized a series of benzamide 3,5-disubstituted analogues and evaluated them for GK activation activity. These analogues showed considerable antihyperglycemic activity in the animal models (Grewal *et al.* 2019). In a study, Charaya *et al.* synthesized thiazole-2-yl benzamide derivatives from benzoic acid and evaluated them for GK activation activity (Charaya *et al.* 2018). A benzamide derivative PF-04937319 (**1**) is under phase-1 clinical trial for the treatment of diabetes.



On the basis of previously synthesized compounds (Park 2012; Park *et al.* 2013), structure-based drug design was performed with pharmacophore development, 3D QSAR, and docking simulations for the determination of potent GK-A by using the PHASE module (Schrodinger). Pharmacophore development determines the important features required for the activity and can be used for 3D QSAR and virtual screening studies. Field and atom-based 3D-QSAR models were developed for the determination of statistical data results of correlation between molecules and their properties. A virtual screening study on the ZINC database generated the potent compounds as GK-A. Docking study revealed the important interactions with amino acids required for activity. On the other hand, the MMGBSA (Molecular Mechanics Generalized Born Surface Area) method was used to predict the binding free energy of the docked molecules. The current findings of the study may be utilized as a guiding tool for the development of novel and effective GK-A.

## 2. Methodologies

### 2.1. Software

The 3D-QSAR, pharmacophore modeling and docking were performed by Schrodinger module (Park *et al.* 2014; Park *et al.* 2015).

### 2.2. Dataset

A dataset of 43 benzamide derivatives was taken for the development of pharmacophore, 3D-QSAR, virtual screening, and docking studies (Table 1). The  $IC_{50}$  values taken from biological activities were converted into  $pIC_{50}$ . Data set were divided into active for 'higher activity' and inactive for 'lower activity' compounds and the remaining were counted in the category of intermediate. The alignment on common scaffold of 43 benzamide derivatives is given in Fig. 1A. The PDB ID-3A0I was used for the docking studies. The crystal ligand of this protein used for comparison of docking outcomes are presented in Fig. 1B (Andreoli *et al.* 2014).

### 2.3. Preparation of ligands

The molecular structure of benzamide derivatives was converted from 2D to 3D by using LigPrep of Schrodinger software. The OPLS\_2005 force field was taken for the preparation of ligands. Further, the prepared molecules were taken for 3D-QSAR and docking simulations (Schrodinger 2017; Ali and Ali 2021).

### 2.4. Pharmacophore development

The pharmacophore model was developed by using PHASE module, where all 43 ligands were aligned on common scaffold and generated conformers using the macromodel search method (Ali and Ali 2021). PHASE module consists six different pharmacophore features including hydrogen bond acceptor (HBA), hydrogen bond donor (HBD), aromatic ring, hydrophobic group, positive ionizable, and negative ionizable groups (Rajeswari *et al.* 2014). The maximum number of sites was fixed to 5 which further

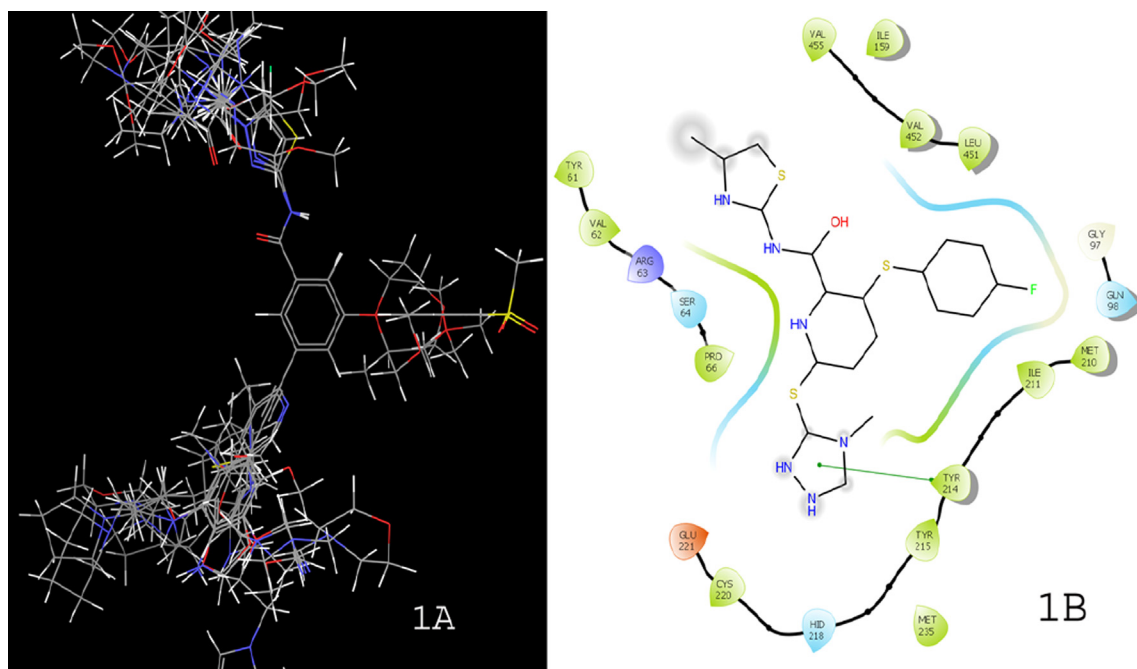
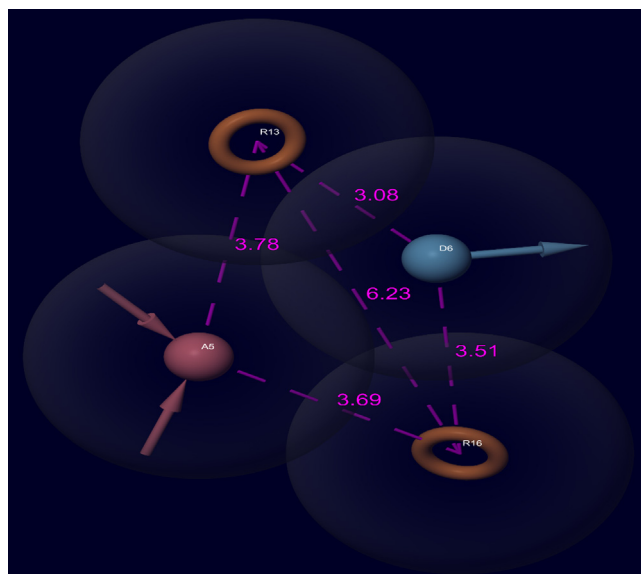


Fig. 1. (1A) Common scaffold alignment of 43 benzamide derivatives; (1B) Binding interactions of crystal ligand with protein 3A0I.

**Table 2**  
The generated pharmacophore hypotheses.

N.	Hypothesis	Phasehypo-S	Survival-S	Inactive-S	Site-S	Vector-S	Volume-S	Selectivity-S
1	DHRR_1	1.25	5.061	1.433	0.689	0.927	0.537	2.063
2	ADRR_1	1.18	5.032	1.234	0.982	0.922	0.409	1.955
3	AHRR_1	1.17	4.964	1.283	0.725	0.957	0.502	1.936
4	AAHRR_1	1.16	4.829	1.329	0.772	0.957	0.521	1.733
5	ADHRR_1	1.15	4.813	1.698	0.775	0.898	0.411	1.775
6	ADHRR_1	1.14	4.805	1.237	0.696	0.926	0.544	1.793
7	ADHRR_2	1.13	4.798	1.269	0.701	0.983	0.465	1.804
8	AAHRR_2	1.11	4.777	1.333	0.607	0.937	0.525	1.864
9	ADHRR_3	1.10	4.764	1.464	0.671	0.961	0.491	1.797
10	AAHRR_1	1.09	4.719	1.298	0.854	0.724	0.481	1.883
11	AADHR_1	1.09	4.713	1.778	0.985	0.951	0.480	1.451
12	HHRR_1	1.09	4.572	1.391	0.742	0.923	0.554	1.509
13	AHHR_1	1.08	4.531	1.129	0.873	0.905	0.545	1.363
14	DHRR_1	1.07	4.524	1.645	0.824	0.846	0.410	1.489
15	AHHR_2	1.07	4.508	1.616	0.740	0.900	0.537	1.485
16	DHHR_1	1.06	4.469	1.513	0.668	0.944	0.548	1.465
17	ADHR_1	1.06	4.459	1.548	0.996	0.928	0.467	1.222
18	AAHR_1	1.06	4.426	1.766	0.995	0.937	0.465	1.183
19	AHRR_1	1.00	4.394	1.683	0.762	0.886	0.409	1.383
20	AHRR_2	0.96	4.389	1.386	0.923	0.695	0.498	1.495

S: Scores



**Fig. 2.** Pharmacophore model (ADRR\_1). Model represents various features by arrow like acceptor (A; pink-colour), donor (D; grey colour), hydrophobic and aromatic ring (R; brown colour) features.

responsible for the generation of the topmost 20 different hypotheses. For the generation of these hypotheses, ligands were categorized into active, inactive, and intermediate.

**Table 3**  
Statistical data generated by atom based (A.B.) and field based (F.B.) models.

P.F.	R <sup>2</sup>		R <sup>2</sup> CV		Q <sup>2</sup>		SD		RMSE		Stability		P-r		F	
	A.B.	F.B.	A.B.	F.B.	A.B.	F.B.	A.B.	F.B.	A.B.	F.B.	A.B.	F.B.	A.B.	F.B.	A.B.	F.B.
1	0.80	0.63	0.59	0.40	0.41	0.72	0.59	0.55	1.06	0.65	0.89	0.91	0.67	0.88	81.90	41.30
2	0.95	0.86	0.57	0.54	0.45	0.61	0.57	0.56	1.02	0.77	0.63	0.77	0.75	0.82	195.20	71.20
3	0.98	0.94	0.59	0.61	0.50	0.69	0.59	0.31	0.97	0.69	0.63	0.72	0.80	0.87	251.20	124.50
4	0.99	0.98	0.62	0.64	0.52	0.71	0.62	0.19	0.96	0.66	0.65	0.70	0.82	0.86	299.80	271.90

P.F.: PLS factor; A.B.: Atom based; F.B.: Field based

The active ligand was set as for those which had pIC<sub>50</sub> value of more than 8 whereas inactive ligands considered for those had pIC<sub>50</sub> value less than 6.6, except these all-other ligands were set as intermediates. The final data consisted of 9 actives and 14 inactive ligands. The hypothesis was generated by using 9 actives and 1 Å box size and 2 Å site distance. The all-generated hypotheses were ranked based on different scores depicted in Table 2 (Crisan et al. 2019; Sakkiah et al. 2014). The hypothesis ADRR\_1 (Fig. 2) showed the top scoring features with one HBA, one HBD, and two aromatic rings. The hypothesis determines the essential features required for the binding with receptor for a particular activity. A total of 20 pharmacophore hypotheses were developed which were ranks according to the score hypothesis (Table 2).

## 2.5. 3D-QSAR

3D-QSAR models were developed by two techniques known as field-based and atom-based QSAR. The developed models showed the essential parameters required for activity by correlating the structure features with biological activity. All 43 benzamide derivatives were separated into a training set with 75% and test set with 25% compounds using 4 PLS factors (Kar et al. 2010). Best models were generated by QSAR models (atom and field-based) described in Table 3. Statistics for atom-type fraction and field type fraction were summarized in Tables 4 and 5. In the atom-based model, 35 molecules were selected for the training, and 8 molecules for the test set, whereas in field-based 31 and 12 molecules were taken for the training and the test set, respectively (Table 6).

**Table 4**

Statistical fraction data procured from atom based model.

Factors	Hydrogen donor	Hydrophobic group	Positive group	Electron withdrawing group	Other
1	0.013	0.675	0.247	0.065	0.013
2	0.012	0.700	0.243	0.044	0.012
3	0.012	0.703	0.241	0.045	0.012

**Table 5**

Statistical fraction data procured from field based model.

Factors	Steric	Electrostatic	Hydrophobic	Hydrogen Acceptor	Hydrogen Donor
1	0.361	0.101	0.242	0.226	0.07
2	0.411	0.098	0.262	0.151	0.077
3	0.403	0.099	0.276	0.138	0.085

The contour maps generated by atom-based and field-based models are presented in Figs. 3 and 4, respectively. These maps are represented as hydrophobic, steric, donor, acceptor, and electrostatic fields (Peng et al. 2017).

## 2.6. Target protein prediction

The potent compounds of the series were selected and submitted to the Swiss-Target-Prediction tool. The said tool predicted var-

**Table 6**The IC<sub>50</sub> value (Actual vs predicted) generated by atom-based and field-based 3D-QSAR model using PLS factor 4.

N.	Ligand	QSAR set (A.B.)	Observed activity	Predicted activity (A.B)	QSAR set (F.B)	Predicted activity (F.B)
1	15b	Training	8.301	6.70	Training	8.49
2	13b1	Training	8.222	6.91	Training	8.18
3	20c1	Training	8.222	7.50	Training	8.32
4	20d1	Training	8.222	8.16	Training	8.17
5	20E_1	Test	8.222	8.16	Test	7.88
6	22c1	Training	8.222	7.29	Test	7.26
7	22d1	Training	8.155	8.12	Training	8.16
8	18g	Test	8.097	7.92	Training	8.01
9	20h1	Test	8.046	7.17	Test	7.47
10	18b1	Training	7.921	7.76	Training	8.05
11	22E_1	Training	7.796	7.85	Training	7.60
12	20f1	Training	7.699	7.50	Training	7.88
13	18a1	Training	7.678	7.69	Training	7.73
14	16c1	Training	7.602	7.29	Training	7.29
15	19	Training	7.569	7.60	Test	7.76
16	18c1	Training	7.523	7.66	Test	7.43
17	18h	Training	7.481	7.25	Training	7.32
18	18d1	Test	7.468	7.35	Training	7.62
19	20a1	Training	7.432	7.52	Training	7.53
20	20g1	Training	7.409	7.42	Test	7.16
21	21	Training	7.409	7.43	Training	7.23
22	22b1	Training	7.337	7.30	Training	7.16
23	22a1	Training	7.276	7.28	Training	7.41
24	16a	Training	7.02	6.89	Training	6.92
25	15a	Test	6.987	6.87	Training	6.69
26	18j	Training	6.975	6.34	Test	6.62
27	20b1	Training	6.788	6.64	Training	6.99
28	18b	Training	6.674	6.76	Test	6.24
29	16b	Training	6.62	6.38	Training	6.23
30	16b1	Training	6.521	6.35	Training	6.18
31	19e	Test	6.502	6.60	Training	6.48
32	19d	Training	6.356	6.27	Training	6.31
33	18i	Training	6.334	6.32	Training	6.33
34	18c	Test	6.162	6.25	Test	5.16
35	19a	Training	6.093	6.29	Training	5.99
36	13a1	Training	5.728	6.01	Training	5.86
37	18d	Training	5.614	5.57	Test	6.09
38	18e	Training	5.127	5.03	Test	4.65
39	16a1	Training	5.114	6.72	Training	5.23
40	18a	Training	4.301	4.18	Test	5.70
41	18f	Training	4.301	5.47	Training	4.45
42	18k	Test	4.301	5.69	Training	4.37
43	19b	Training	4.301	5.23	Training	4.44

A.B.: Atom based; F.B.: Field based

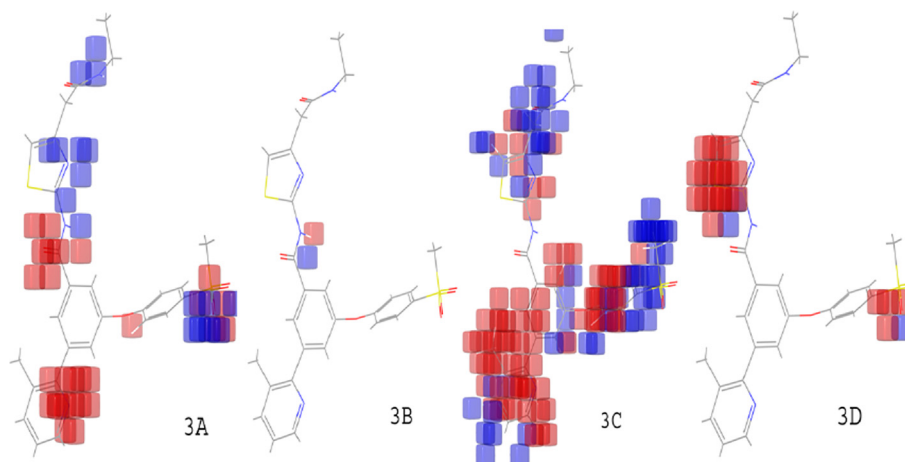


Fig. 3. 3D contour maps, atom-based: (3A) EWG; (3B) HBD group; (3C) Hydrophobic group; (3D) Positive ionic group.

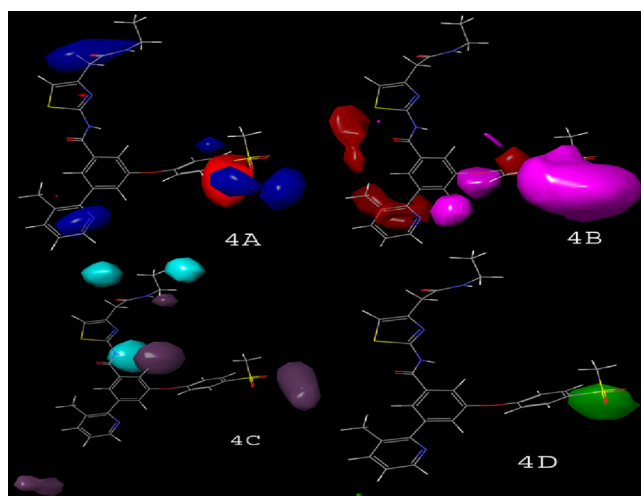


Fig. 4. Different field contour maps: (4A) Electrostatic (blue {favored}, red {disfavored}); (4B) HBA (red {favored}, magenta {disfavored}); (4C) HBD (purple {favored}, cyan {disfavored}); (4D) Steric (green {favored}, yellow {disfavored}).

Table 7

Docking scores generated through the Glide module.

N.	Ligand	D.S. (XP) kcal/mol	D.S. (SP) kcal/mol	N.	Ligand	DS (XP) kcal/mol	DS (SP) kcal/mol
1	18d	-8.854	-12.715	23	19d	-10.014	-9.62
2	19b	-10.686	-12.412	24	13a1	-11.856	-9.56
3	19e	-11.07	-11.731	25	13b1	-10.242	-9.519
4	19a	-10.768	-11.467	26	18b	-10.21	-9.396
5	16b	-9.207	-11.361	27	18a	-9.761	-9.059
6	16a	-9.261	-11.296	28	19	-8.507	-9.03
7	15a	-9.351	-11.284	29	18b1	-8.284	-9.001
8	18k	-9.258	-11.149	30	18d1	-9.406	-8.769
9	15b	-9.047	-11.088	31	20d1	-9.615	-8.707
10	18h	-8.742	-10.866	32	22b1	-8.48	-8.701
11	18c	-8.522	-10.622	33	20h1	-11.053	-8.694
12	18e	-7.234	-10.615	34	16b1	-8.827	-8.653
13	20E_1	-8.191	-10.613	35	20c1	-8.548	-8.653
14	18f	-9.513	-10.536	36	20g1	-8.464	-8.57
15	18g	-11.172	-10.443	37	22a1	-7.801	-8.548
16	18j	-7.131	-10.427	38	16a1	-12.379	-8.513
17	18i	-9.313	-10.184	39	22E_1	-9.187	-8.274
18	18a1	-10.037	-9.95	40	22c1	-7.757	-7.804
19	20a1	-8.082	-9.897	41	20b1	-5.211	-7.388
20	18c1	-11.886	-9.767	42	20f1	-10.515	-6.959
21	16c1	-10.364	-9.703	43	22d1	-7.929	-6.476
22	21	-8.751	-9.679				

DS: Docking score; Extra precision: XP; SP: Standard precision.

ious protein targets, in which GK-A was the most appropriate target for the selected molecules.

### 2.7. Docking analysis

The PDB ID-3AOI consists a three-dimensional structure of GK-A and was downloaded through protein data bank (Tagami et al. 2010). The docking study was performed to determine the binding scores between ligand and receptor by using the Glide module. The SP and XP methodologies were used for all 43 ligands with PDB ID-3AOI (Table 7). The MMGBSA based rescoring technique was used for the prediction of binding free energy calculation between ligands and receptor molecule (Table 8). However, DFT studies can give more accurate assessment of binding/docking (Van Mourik et al., 2014).

### 2.8. ADME prediction studies

The top scored compounds were analyzed by different ADME properties such as drug-likeness, solubility, and pharmacokinetic

**Table 8**

The scores calculated by different docking methodologies used in the present study with their rescoring values calculated by MMGBSA method.

C	PDB ID: 3A0I			
	D.S. (XP) kcal/mol	D.S. (SP) kcal/mol	D.S. (HTVS) kcal/mol	dG bind kcal/mol
18g	-11.172	-10.443	-10.65	-81.31
13b1	-10.242	-9.519	-7.85	-74.62
19e	-11.07	-11.73	-6.38	-83.57
19a	-10.77	-11.47	-9.26	-80.57
16b	-9.21	-11.36	-10.78	-84.33
16a	-9.26	-11.30	-11.47	-81.96
15b	-9.05	-11.09	-9.24	-89.31
ARRY-403	-10.259	-10.101	-9.26	-72.62
RO-530552	-6.707	-9.074	-7.75	-39.15
Piragliatin	-8.345	-8.144	-7.24	-39.35
Glucokinase activator 1	-3.36	-5.782	-8.37	-0.96
ZINC08974524	-8.43	-11.17	-10.26	-19.55
ZINC00656909	-8.715	-10.887	-8.62	-56.96
ZINC31812808	-8.40	-8.223	-9.37	-76.4
ZINC14791611	-8.294	-10.879	-8.28	-29.58
ZINC05204145	-7.984	-7.323	-8.32	-53.31
ZINC01114130	-7.854	-10.21	-9.65	-37.62
ZINC09712705	-7.764	-8.962	-9.78	-47.96
ZINC14462664	-7.65	-10.997	-7.47	-75.4
ZINC02474054	-6.186	-4.208	-6.25	-8158

D.S.: Docking score; XP: Extra precision; SP: Standard precision; HTVS: High-throughput virtual screening.

studies. The QikProp software was used to calculate ADME properties (Table 9). Further, the Swiss-ADME tool was used to evaluate additional parameters like cytochrome profile of the drug with permeation through different other barriers.

### 3. Results

#### 3.1. Analysis of pharmacophore modeling

The generated pharmacophore hypotheses with different scores are presented in Table 2. The hypothesis ADRR\_1 was chosen as the best hypothesis with phase hypo-score = 1.18, survival score = 5.03, and site score = 0.98. The field-based and atom-based QSAR studies showed reliable statistical parameters with different evaluation factors. The results showed internal validation parameters such as  $R^2$  values 0.99, 0.98;  $R^2CV$  values 0.62, 0.64;  $Q^2$  values 0.52, 0.71; SD values 0.62, 0.19; RMSE values 0.96, 0.66 and F values 299, 271 for atom-based and field-based models, respectively (Table 3). The scatter plots for both models are shown in Fig. 5.

**Table 9**

ADME predictions of top scored compounds.

C	QP log Po/w <sup>1</sup>	QPP- Caco <sup>2</sup>	QP log B.B. <sup>3</sup>	QPP-MDCK <sup>4</sup>	QP log Kh <sub>sa</sub> <sup>5</sup>	MetR <sup>6</sup>	PHOA <sup>7</sup>
18g	3.524	62.806	-1.768	46.094	0.214	6	66.803
13b1	3.606	2683.955	-0.698	1438.153	-0.05	3	100
19e	3.411	290.144	-2.14	130.171	-0.097	4	78.033
19a	3.746	323.686	-1.674	146.509	0.346	2	93.806
16b	3.784	251.098	-1.595	332.05	0.266	3	92.054
16a	3.544	300.192	-1.505	262.463	0.187	3	92.039
15b	3.472	76.153	-1.903	56.786	-0.114	7	67.996
ARRY-403	2.664	170.959	-1.879	200.448	-0.156	6	82.508
GK-A 1	4.515	22.249	-2.361	47.821	0.115	3	64.54
Piragliatin	3.048	435.091	-1.217	374.987	0.038	7	92.016
RO-530552	2.775	199.82	-2.015	174.056	-0.177	4	84.373
ZINC08974524	4.32	2282.231	-0.392	2329.878	0.362	4	100

Predicted [1: Octanol/water partition coefficient; 2: Caco-2 cell permeability (nm/s); 3: Brain/blood partition coefficient; 4: Apparent MDCK cell permeability (nm/s); 5: Human serum albumin binding; 6: Number of metabolic reactions; 7: Percent human oral absorption.

#### 3.2. 3D-QSAR

The contour maps showed the correlation between different bioactivities by various substituents on the core moiety (Fig. 3). The correlation between actual and predicted activities of test and training-set compounds for atom-based QSAR is depicted in Fig. 5. The contour maps generated by field-based model include HBA, HBD, steric, electrostatic, and hydrophobic fields (Fig. 4). Different substituent groups on the potent compound (16a) described by various colour responsible for increase or decrease in activity. The correlation between actual and predicted activities of test and training-set compounds for field-based QSAR is depicted in Fig. 5.

#### 3.3. Docking and virtual screening studies

The PDB ID-3A0I was taken for docking purposes to evaluate binding interactions of potent ligands and ZINC compounds. The docking scores were compared with the observed activity. Compounds, 18g, 13b1, 19e, 19a, 16b, 16a, and 15b showed binding



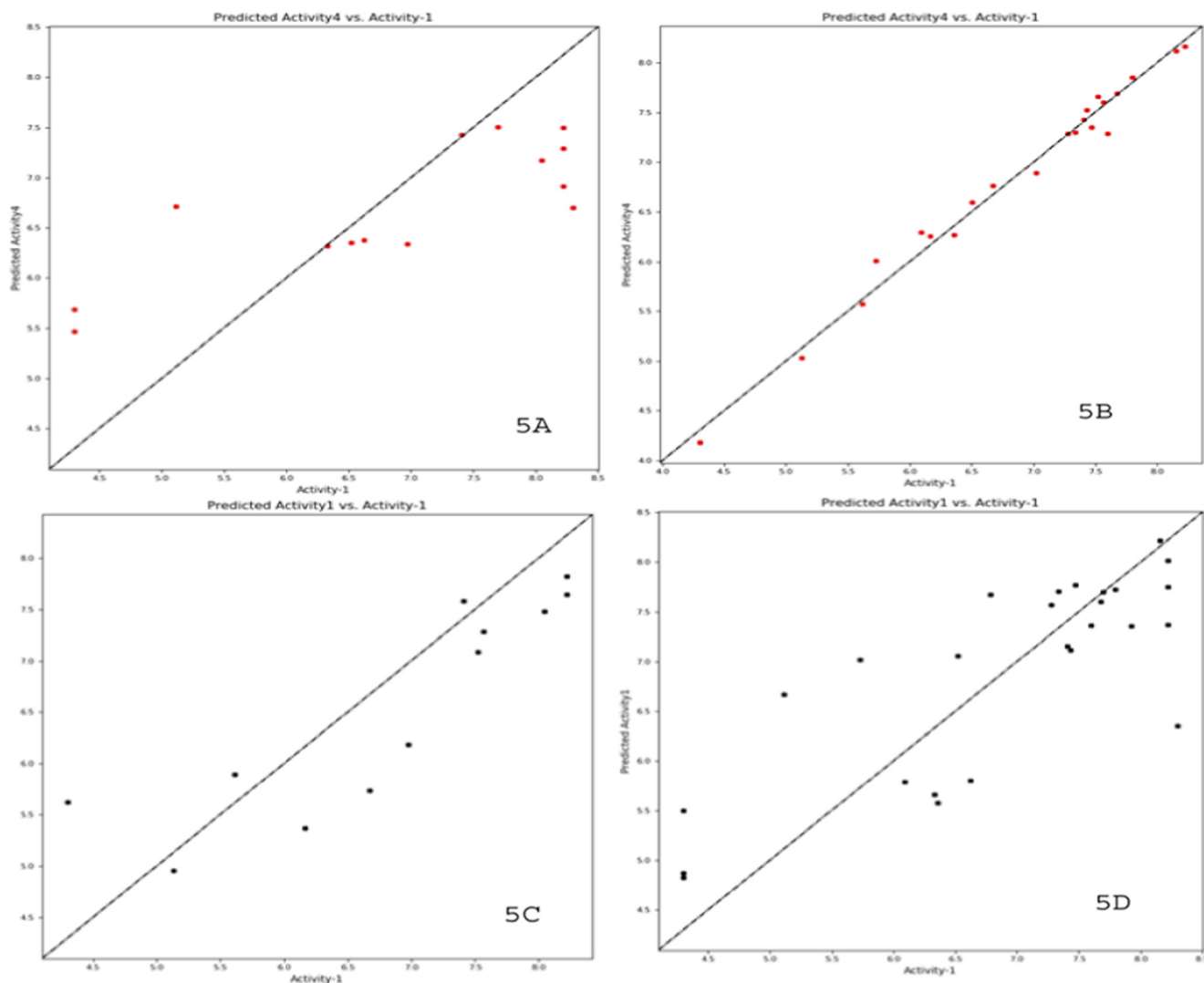


Fig. 5. Correlation between test (5 A & C) and training (5B & D) set compounds by using atom and field-based 3D QSAR models.

interactions with important amino acids required for GK-A. The amino acids bind with both compounds 15b and 18g were ARG250 and THR65, ARG63 as shown in Fig. 6. Compound 16a also showed good binding interactions described in Fig. 7. The docking score of the potent compounds of the series compared with standard drugs such as glucokinase activator 1, piragliatin, ARRY-403, and RO-530552 are described in Table 8. The binding interactions of other potent compounds 19e and 19 are displayed in Fig. 8.

### 3.4. MMGBSA-based rescoring

The rescoring of docked structure of ligand and protein was performed by the MMGBSA-based method (molecular mechanics energies combined with the Poisson–Boltzmann or generalized Born and surface area continuum solvation). The screened ZINC hit compound ZINC08974524 (complex of ZINC08974524: 3A0I) showed docking score of  $-8.428$  kcal/mol. Other ZINC hits such as ZINC00656909, ZINC31812808, ZINC14791611, ZINC05204145, ZINC01114130, ZINC09712705 and ZINC14462664 showed XP docking scores  $-8.715$ ,  $-8.40$ ,  $-8.294$ ,  $-7.984$ ,  $-7.854$ ,  $-7.764$  and  $-7.65$  kcal/mol, respectively. All ZINC compounds showed negative value of  $dG$  binding energies as compared with standards (Table 8).

### 3.5. ADME properties calculation

ADME properties were calculated by the QikProp module, comprise of one another SwissADME tool. These parameters were within the acceptable range for ligands and ZINC hits (Table 9). The compounds of the series showed drug-likeness properties with no violation of the Lipinski rule. The bioavailability score of compounds showed the value of 0.55.

## 4. Discussion

The final hypothesis consisted of one HBD, one HBA, and two aromatic ring structures. The hypothesis (ADRR\_1) showed alignment with other molecules of the series and displayed good correlation between structure and bioactivity. The features of the hypothesis were further taken for screening of ZINC compounds from the ZINCPharmer (<http://zincpharmer.csb.pitt.edu/>) online tool. The atom based QSAR maps indicated the influence on bioactivity by the addition of substituents on the nucleus. The blue contour maps showed an increase in activity, whereas red maps showed decrease in activity. The compound 16a showed alignment with pharmacophore hypothesis ADRR\_1 with different colours on their substituents. The electron-withdrawing group (EWG) substi-

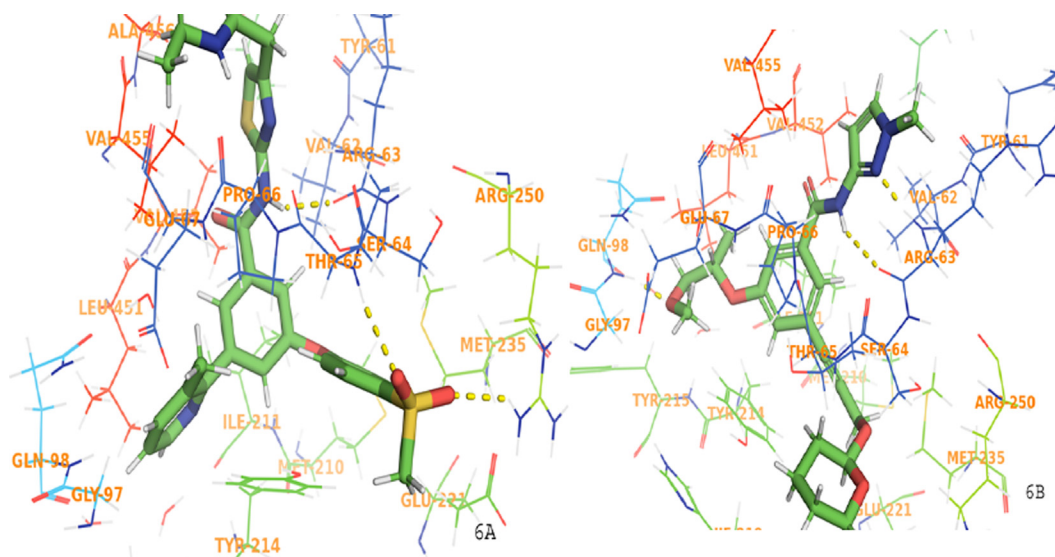


Fig. 6. Ligand interaction diagram for higher scoring compound 15b (6A) and 18 g (6B) in docking study.

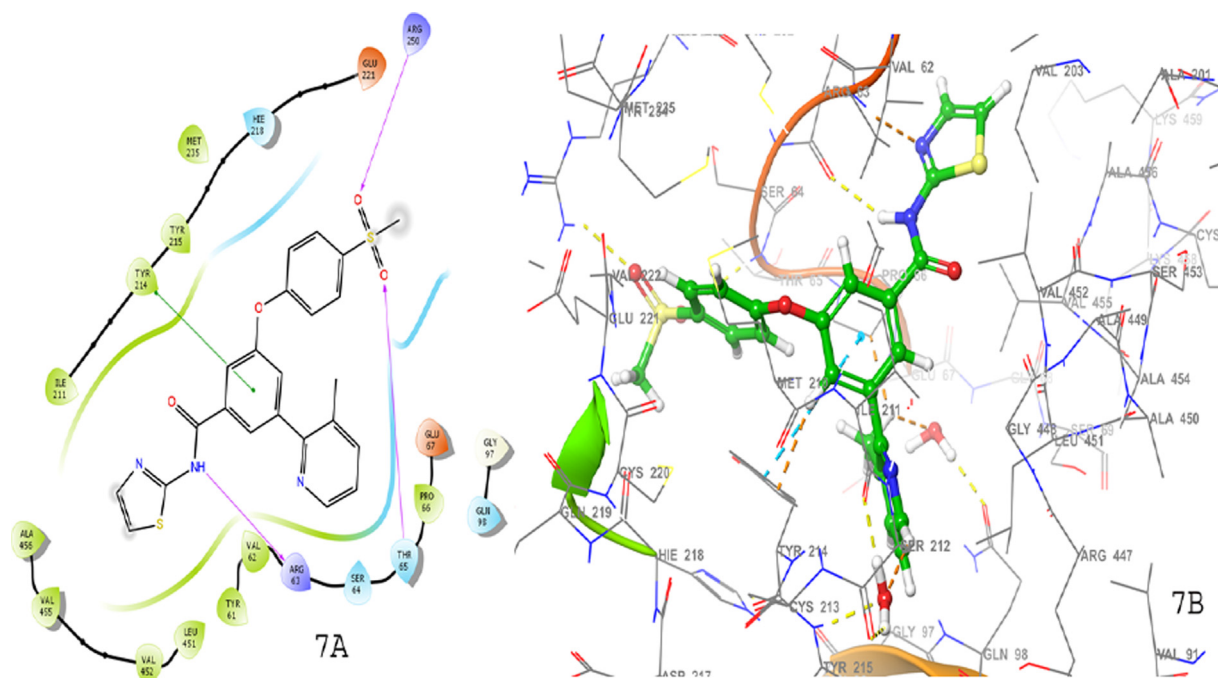


Fig. 7. (7A) 2D and (7B) 3D docking interactions represented by compound 16a.

tution on benzamide derivatives exhibited increase in the activity, whereas EWG substitution on phenyl ring showed decrease in activity, as represented by red maps (Fig. 3). The HBD group addition showed no changes in activity. The hydrophobic group addition connected to the amide group displayed increase in activity, whereas the introduction of such group at phenyl ring decreased the potency and showed mixed activity throughout the ring. However, the addition of positive and negative ionic groups showed decrease in the activity.

In field based QSAR contour map electrostatic group contains the blue colour at the amide group linked heterocyclic compounds that showed the introduction of electron positive group at the site responsible for increase in the activity. The phenyl ring connected to heterocyclic ring with electron positive group may decrease or increase the activity. The HBA group introduction at phenyl ring

connected group may increase the activity. The addition of HBD group at the amide group may increase the activity. The group contains steric field with green color in phenyl ring substituted group may be responsible for increase in activity. The potent compound 15b of the series showed good docking score using interactions with amino acid residues (NH...ARG63), (SO<sub>2</sub>...ARG250, THR65), and  $\pi$ - $\pi$  stacking with (phenyl...TYR214). Compound 16a also showed good binding interactions with amino acid residues such as TRY214, ARG250, THR65, and ARG63 (docking score  $-11.296$  kcal/mol), important for GK-A activity (Fig. 7). The docking scores and the amino acid residues of the potent compounds of the series compared with standard drugs such as glucokinase activator 1 ( $-3.36$  kcal/mol), piragliatin ( $-8.345$  kcal/mol), ARRY-403 ( $-10.259$  kcal/mol), and RO-530552 ( $-6.707$  kcal/mol) (Table 8). Furthermore, the other potent compounds 19e and 19



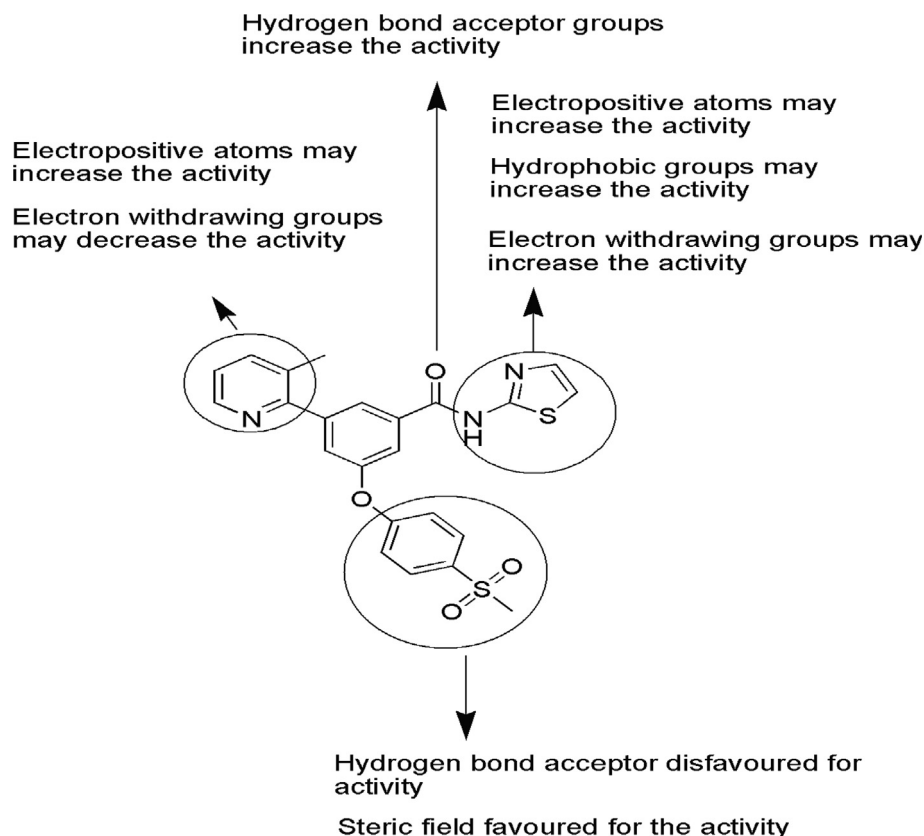


**Fig. 10.** Substitutions on benzamide scaffold with different characteristic features for the development of future compounds as GK-A.

base showed good ADME properties (Table 9). However, cytochrome profiling for ZINC hits shown inhibitory activities against CYP3A4, CYP2C19, and CYP2C9. All the compounds of the series and ZINC hits showed noncarcinogenic activities.

## 5. SAR optimization

The pharmacophore model, 3D QSAR, virtual screening, and Zinc hit compounds may be used as a basis for the production of novel compounds as GK-A depicted in Fig. 10. The present SAR optimized by the 3D QSAR study revealed that the substitutions on benzamide scaffold with different characteristic features for the development of novel GK-A. The core moiety in the place of thiazole ring can be replaced by some electropositive atoms and hydrophobic groups such as long carbon chain and phenyl ring responsible for increase in activity. The oxygen atom of the benzamide group is more prominent for activity, or if it is replaced by less electronegative groups such as sulphur or nitrogen, then the activity may be diminished. The pyridine ring connected to the benzamide scaffold can be replaced by electropositive groups that results an increase in activity. These features can be used for the further development and synthesis of novel derivatives as GK-A.

## 6. Conclusion

The present manuscript revealed a computation study on benzamide derivatives processed in a sequence to produce potent GK-As, where ligands and ZINC hits showed no violation of the Lipinski rules. All screened compounds displayed good synthetic accessibility. Based on 3D-QSAR, pharmacophore development, SwissTargetPrediction, virtual screening, and molecular docking

studies, we may design novel molecules with good ADME properties and low toxicity. ADRR\_1 is determined as the best pharmacophore in the study. The 3D QSAR study showed the best statistical data by atom-based and field-based models, consecutively. The binding interactions of compounds showed important amino acids required for activity. Fig. 10 showed the importance of different substituents on core moiety which may help for the development of novel compounds as GK-A. Furthermore, the present study may be helpful for researchers as a guiding tool for the development of novel benzamide derivatives as GK-A.

## Declaration of Competing Interest

The author declare that there is no known competing financial interests or personal relationships that could have appeared to influence the work reported in this paper.

## Acknowledgment

Dr Amena Ali is thankful for Schrödinger team for training and license. This research received no grant.

## References

- Ali, A., Ali, A., 2021. Integrated computational approaches on pyrazoline derivatives as B-Raf kinase inhibitors for the development of novel anticancer agents. *J. Mol. Struct.* 1230, 129861. <https://doi.org/10.1016/j.jmolstruc.2020.129861>.
- American Diabetes Association, 2009. Diagnosis and classification of diabetes mellitus. *Diabetes Care.* 32, S62–S67.
- Andreoli, M., Persico, M., Kumar, A., Orteca, N., Kumar, V., Pepe, A., Mahalingam, S., Alegria, A.E., Petrella, L., Sevcunaita, L., Camperchioli, A., Mariani, M., Di Dato, A., Novellino, E., Scambia, G., Malhotra, S.V., Ferlini, C., Fattorusso, C., 2014.

- Identification of the first inhibitor of the GBP1:PIM1 interaction. Implications for the development of a new class of anticancer agents against paclitaxel resistant cancer cells. *J. Med. Chem.* 57 (19), 7916–7932.
- Antoine, M., Boutin, J.A., Ferry, G., 2009. Binding kinetics of glucose and allosteric activators to human glucokinase reveal multiple conformational states. *Biochemistry* 48, 5466–5482.
- Bebornitz, G.R., Beaulieu, V., Dale, B.A., Deacon, R., Duttaroy, A., Gao, J., Grondine, M. S., Gupta, R.C., Kakmak, M., Kavana, M., Kirman, L.C., Liang, J., Maniara, W.M., Munshi, S., Nadkarni, S.S., Schuster, H.F., Stams, T., Denny, I.S., Taslimi, P.M., Vash, B., Caplan, S.L., 2009. Investigation of functionally liver selective glucokinase activators for the treatment of type 2 diabetes. *J. Med. Chem.* 52, 6142–6152.
- Charaya, N., Pandita, D., Grewal, A.S., Lather, V., 2018. Design, synthesis and biological evaluation of novel thiazol-2-yl benzamide derivatives as glucokinase activators. *Comput. Biol. Chem.* 73, 221–229.
- Crisan, L., Borota, A., Bora, A., Pacureanu, L., 2019. Diarylthiazole and diarylimidazole selective COX-1 inhibitor analysis through pharmacophore modeling, virtual screening, and DFT-based approaches. *Struc. Chem.* 30, 2311–2326.
- Grewal, A.S., Kharb, R., Prasad, D.N., Dua, J.S., Lather, V., 2019. Design, synthesis and evaluation of novel 3,5-disubstituted benzamide derivatives as allosteric glucokinase activators. *BMC Chem.* 13, 1–14.
- Kar, S., Harding, A.P., Roy, K., Popelier, P.L.A., 2010. QSAR with quantum topological molecular similarity indices: toxicity of aromatic aldehydes to *Tetrahymena pyriformis*. *SAR QSAR Environ. Res.* 21, 149–168.
- Mao, W., Ning, M., Liu, Z., Zhu, Q., Leng, Y., Zhang, A., 2012. Design, synthesis, and pharmacological evaluation of benzamide derivatives as glucokinase activators. *Bioorg. Med. Chem.* 20, 2982–2991.
- Massa, M.L., Gagliardino, J.J., Francini, F., 2011. Liver glucokinase: An overview on the regulatory mechanisms of its activity. *IUBMB Life.* 63, 1–6.
- Matschinsky, F.M., Porte, D., 2010. Glucokinase activators (GKAs) promise a new pharmacotherapy for diabetics. *F1000 Med. Rep.* 2, 43.
- Matschinsky, F.M., 1996. A lesson in metabolic regulation inspired by the glucokinase glucose sensor paradigm. *Diabetes* 45, 223–241.
- Park, K., 2012. Identification of YH-GKA, a novel benzamide glucokinase activator as therapeutic candidate for type 2 diabetes mellitus. *Arch. Pharm. Res.* 35, 2029–2033.
- Park, K., Lee, B.M., Hyun, K.H., Han, T., Lee, D.H., Choi, H.H., 2015. Design and synthesis of acetylenyl benzamide derivatives as novel glucokinase activators for the treatment of T2DM. *ACS Med. Chem. Lett.* 6, 296–301.
- Park, K., Lee, B.M., Hyun, K.H., Lee, D.H., Choi, H.H., Kim, H., Chong, W., Kim, K.B., Nam, S.Y., 2014. Discovery of 3-(4-methanesulfonylphenoxy)-N-[1-(2-methoxy-ethoxymethyl)-1H-pyrazol-3-yl]-5-(3-methylpyridin-2-yl)-benzamide as a novel glucokinase activator (GKA) for the treatment of type 2 diabetes mellitus. *Bioorg. Med. Chem.* 22 (7), 2280–2293.
- Park, K., Lee, B.M., Kim, Y.H., Han, T., Yi, W., Lee, D.H., Choi, H.H., Chong, W., Lee, C.H., 2013. Discovery of a novel phenylethyl benzamide glucokinase activator for the treatment of type 2 diabetes mellitus. *Bioorg. Med. Chem. Lett.* 23, 537–542.
- Peng, X.X., Feng, K.R., Ren, Y.J., 2017. Molecular modeling studies of quinazolinone derivatives as novel PI3Kd selective inhibitors. *RSC Adv.* 7, 56344–56358.
- Pfefferkorn, J.A., Guzman-Perez, A., Oates, P.J., Litchfield, J., Aspnes, G., Basak, A., Benbow, J., Berliner, M.A., Bian, J., Choi, C., Freeman-Cook, K., Corbett, J.W., Didiuk, M., Dunetz, J.R., Filipinski, K.J., Hungerford, W.M., Jones, C.S., Karki, K., Ling, A., Li, J.-C., Patel, L., Perreault, C., Risley, H., Saenz, J., Song, W., Tu, M., Aiello, R., Atkinson, K., Barucci, N., Beebe, D., Bourassa, P., Bourbonnais, F., Brodeur, A.M., Burbey, R., Chen, J., D'Aquila, T., Derksen, D.R., Haddish-Berhane, N., Huang, C., Landro, J., Lee Lapworth, A., MacDougall, M., Perregaux, D., Pettersen, J., Robertson, A., Tan, B., Treadway, J.L., Liu, S., Qiu, X., Knafels, J., Ammirati, M., Song, X.i., DaSilva-Jardine, P., Liras, S., Sweet, L., Rolph, T.P., 2011. Designing glucokinase activators with reduced hypoglycemia risk: discovery of N, N-dimethyl-5-(2-methyl-6-((5-methylpyrazin-2-yl)-carbamoyl)benzofuran-4-yloxy)pyrimidine-2-carboxamide as a clinical candidate for the treatment of type 2 diabetes mellitus. *Med. Chem. Commun.* 2 (9), 828. <https://doi.org/10.1039/c1md00116g>.
- Pfefferkorn, J.A., Guzman-Perez, A., Litchfield, J., Aiello, R., Treadway, J.L., Pattersen, J., et al., 2012. Discovery of (S)-6-(3-cyclopentyl-2-(4-(trifluoromethyl)-1H-imidazol-1-yl)propanamido)nicotinic acid as a hepatoselective glucokinase activator clinical candidate for treating type 2 diabetes mellitus. *J. Med. Chem.* 55, 1318–1333.
- Rajeswari, M., Santhi, N., Bhuvanawari, V., 2014. Pharmacophore and Virtual Screening of JAK3 inhibitors. *Bioinfo.* 10, 157–163.
- Sakkiah, S., Senese, S., Yang, Q., Lee, K.W., Torres, J.Z., 2014. Dynamic and multi-pharmacophore modeling for designing polo-box domain inhibitors. *PLoS One* 9, e101405.
- Schrodinger. 2017. LigPrep, Schrodinger, LLC, NY.
- Tagami, S., Sekine, S., Kumarevel, T., Hino, N., Murayama, Y., Kamegamori, S., Yamamoto, M., Sakamoto, K., Yokoyama, S., 2010. Crystal structure of bacterial RNA polymerase bound with a transcription inhibitor protein. *Nature* 468, 978–982.
- Van Mourik, T., Bühl, M., Gaigeot, M.P., 2014. Density functional theory across chemistry, physics and biology. *Philosophical Trans. Ser. A, Math. Phys. Eng. Sci.* 372 (2011), 20120488.
- Waring, M.J., Brogan, I.J., Coghlan, M., Johnstone, C., Jones, H.B., Leighton, B., McKerrecher, D., Pikea, K.G., Robba, G.R., 2011. Overcoming retinoic acid receptor- $\alpha$  based testicular toxicity in the optimisation of glucokinase activators. *Med. Chem. Commun.* 2, 771–774.